Integrated Wire Grid Polarizer and Plasmonic Polarization Beam Splitter

A. Melikyan[1,2], C. Gaertner[1,2], K. Koehnle[1,2], A. Muslija[1,2], M. Sommer M. Kohl[1,2], C. Koos[1,2], W. Freude[1,2], J. Leuthold[1,2]

1: Institute of Photonics and Quantum Electronics, Karlsruhe Institute of Technology, Karlsruhe, Germany,
2: Institute of Microstructure Technology, Karlsruhe Institute of Technology, Karlsruhe, Germany,
Author e-mail address: argishti.melikyan@kit.edu

Abstract: An ultra-compact, low loss, high extinction ratio polarization beam splitter is proposed for the SOI platform. The device is 3.5 μm in length and provides more than 11dB extinction ratio with less than 1dB plasmonic losses.

OCIS codes: (250.5403) Plasmonics; (130.5440) Polarization-selective devices;

1. Introduction

Ultra-compact, lowest loss polarization beam splitters (PBSs) are vital elements that are needed if CMOS compatible silicon photonics is going to be deployed. The reason for the small footprint requirements on photonics are simply because of the expensive cost associated to every square micrometer in a CMOS fab. Moreover, for the next generation of optical interconnects between chips employing polarization and wavelength diversity schemes, PBSs should provide broadband operation through the entire communication window. In the meantime, they should be simple to fabricate and compatible with silicon photonics.

Conventionally, polarization beam splitter cubes have been widely used for polarization multiplexed and demultiplexed systems due to their high extinction ratio (ER) and broadband operation [1]. Nowadays, they can provide more than 20dB extinction ratio in the entire communication wavelength window. Another historical approach to separate two orthogonal polarizations is wire grid polarizer (WGP) first time reported by Heinrich Hertz at 1888 for radio waves and then converted to optical frequencies by C. H. Brown at 1940 [2]. WGPs consists of metallic wires which are separated with a distance smaller than the wavelength of incident electromagnetic (EM) wave. The EM polarized perpendicular to the metallic wire grids can pass through the polarizer, while the EM polarized parallel to the gird is either reflected back or absorbed. However, these devices are bulky and not well appropriate for miniaturized silicon photonics.

More compact PBSs have been proposed making use of e.g. photonic crystals [3-5], directional coupling configuration [6], gratings [7-8], surface plasmon polaritons [9]. However, above devices exceed the footprint of the PBS proposed in this paper and require relatively more complicated fabrication procedure. Recently, a polarization beam splitter consisting of a metal nanoribbon and two dielectric waveguides is proposed and numerically investigated [10]. While the length of the PBS is shorter than 3μm its fabrication issues concerning to the enormous aspect ratio of silver nanoribbon is still to be solved.

Here, we propose new, simple to fabricate, integrated plasmonic PBS with an ultra-compact size of 3.5 μm providing high extinction ratio. Our PBS is compatible with the standard SOI platform. The scheme takes advantage of the fact that two orthogonal polarizations can efficiently be separated with negligible losses by making use of a vertical slot plasmonic waveguide. The device operation principle is similar to the wire grid polarizers and provides broadband performance. Unlike to other approaches found in literature, our PBS is void of unnecessary losses, resonant behaviors as well as it is endowed with very high directivity unlike to photonic crystal based polarization beam splitters [3-5],[7-8],[9].

2. Design and Methods

The polarization beam splitter is designed on silicon dioxide substrate, see Figure 1. It consists of two parallel silicon nanowire waveguides (SiWG) with a thickness of 340nm and width of 300nm. They are separated with 200 − 300nm of gap. Between the silicon nanowires a vertical slot plasmonic waveguide (PWG), consisting of two silver rods, is situated. The cladding material is taken to be silicon dioxide with refractive index of 1.44. Similar performance can also be achieved in the case of PMMA cladding, because of similar refractive indices of PMMA and silicon dioxide.

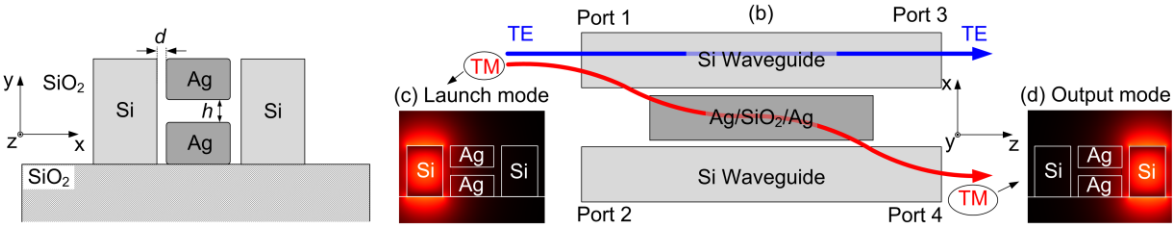

Figure 1: Schematic of polarization beam splitter. (a) Cross section and (b) top view of PBS with PBS with d = 50 nm and h = 50 nm. Launching the TM mode (c) at the Port 1, the light couples to the right SiWG via tunneling through plasmonic slot waveguide and transmits to the Port 4. While TE polarized light launched from the Port 1 transmits through the device almost undisturbed and couples to the Port 3.

When the TE mode at Port 1 is excited, the two metal rods act as one piece, and prevent the wave from coupling to the neighboring WG. Therefore, the TE mode can transmit undisturbed through the device to Port 3. Upon excitation of the TM mode, the wave at the left SiWG can penetrate into the PWG slot and couple to the right SiWG. Thus, in the case of TM excitation the vertical slot serves as a channel between two silicon waveguides. Choosing the right material and geometrical properties the coupling efficiency between the two SiWG for the TM mode can significantly be increased. This then promises high extinction ratio ER = P_{TE} / P_{TM} for the PBS.

For the numerical optimization of the PBS we employ COMSOL Multiphysics. The device length and the coupling efficiency of the TM mode to Port 4 are calculated as follows. First, the TM eigenmode of the left SiWG is simulated (see, Figure 1(c)). Second, the supermodes of the plasmonic section are simulated. Third, the excitation efficiency of each individual supermode with the TM polarized launch field from Port 1 is calculated. The field distribution in the PBS due to the propagation of these supermodes can be represented by

$$\mathbf{A}(x,y,z)=\sum_{\mu=1}^{N} c_\mu a_{1\mu}(x_k,y_k,0)\cdot e^{-j\beta_\mu z} \tag{1}$$

where. c_μ is the excitation efficiency of μ^{th}, $a_{1\mu}(x_k,y_k,0)$ is the analogue of complex electric and magnetic field components and describes the mode profile of the μ^{th} supermode. $\beta_\mu = k_0 n_{eff}$ is the eigenvalue of the μ^{th} mode. In our case, the summation runs through all those modes that have been excited with more than five percent efficiency. The first six supermodes in the plasmonic section are depicted in Figure 2 with their excitation efficiencies c_μ.

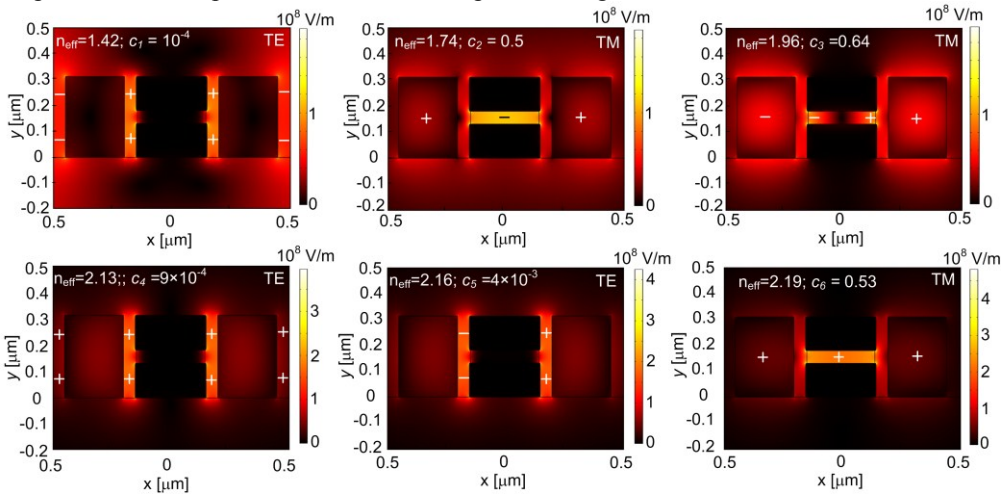

Figure 2. Representative sketch of supermodes at the PBS. The TM excitation efficiency c_μ for the respective supermode is depicted at the top of each plot. The phase of the dominating electric field component (Ey or Ex depending if the mode is quasi-TE or quasi-TM) in the cross section is represented with (+) and (−) signs. The second, the third and the sixth supermodes in the PBS contribute to the coupling of a TM mode from the left SiWG to the right SiWG.

Finally, the normalized overlap integral C_μ between the TM mode of the right SiWG (see Figure 1(d)) and the field distribution $\mathbf{A}(x,y,z)$ of the supermodes is calculated along the L = 20 μm plasmonic section with Δz = 50 nm increments.

$$C_\mu(z_1)=\frac{1}{2}\frac{\mathrm{Re}\left\{\iint\left[E_s(x,y,0)\times H_p^*(x,y,z_1)+H_s(x,y,0)\times E_p^*(x,y,z_1)\right]dxdy\right\}}{\sqrt{P_s\times P_p}} \tag{2}$$

where E_s, H_s are the electric and magnetic field components of the right SiWG mode. E_p and H_p represent the field distribution at the plasmonic section in terms of electric and magnetic fields obtained from Eq. (1). P_s and P_p are the power of the right SiWG mode and at the plasmonic section, respectively. The surface integration has been numerically performed for a 6×6 μm^2 area applying to trapezoidal rule and using non-uniform triangular mesh.

3. Results and Discussion

The maximum overlap integral Eq. (2) along L is considered to be the figure-of-merit of the PBS describing its ER. The PBS length is calculated as half of the length after which the field is coupled back to left SiWG, i.e. half of the beat length. It can be seen that high performance PBS with a length of sub-10 μm are feasible.

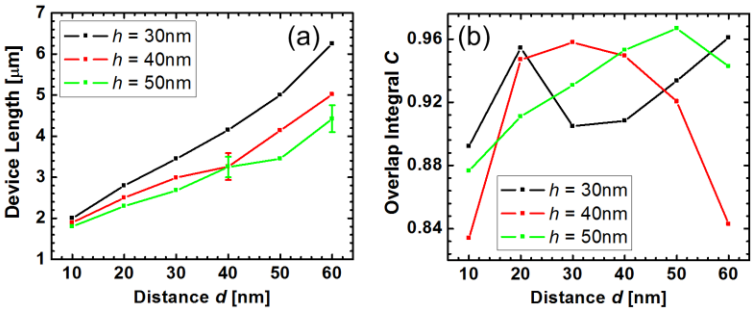

Figure 3. Device length (a) and the maximum overlap integral (b) for various plasmonic slot heights h. Figure 3 (b) shows that efficient tunneling of TM mode of the left SiWG to the right SiWG is feasible in a sub−10μm long device.

To prove the high performance of the PBS as well as to validate above described numerical calculation we have carried out a fullwave simulation on the structure depicted in Figure 2 using CST MWS, see Figure 4. It can be seen that the TM mode excited from left SiWG tunnels through the plasmonic nanoslot and couples to the right SiWG. While TE mode stays in the left SiWG. The small coupling to the right SiWG is due to the field scattering from metal edge. It can easily be avoided with designing 90° bends of SiWGs.

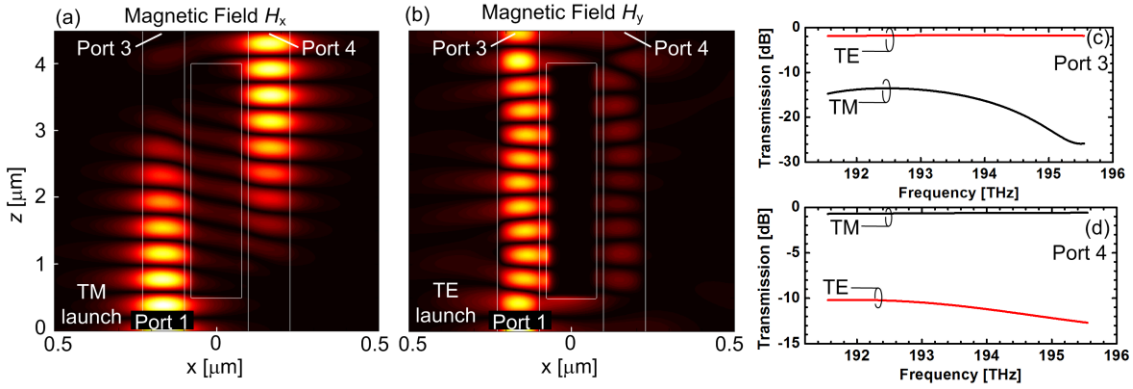

Figure 4. Field distrubtion in the PBS and transmission at the Port 4 and Port 3 for both TM and TE excitations. Magnetic field distrubtion in the PBS for the case of TE (a) and TM (b) excitation. Transmission spectrum at Port 3 (c) and Port 4 (d) for both TE (red) and TM (black) excitations from Port 1. TM polarized light tunnels through the PWG and couples to the neiboring SiWG, while TE mode transmits through the PBS staying in the left arm. More than 11dB extinction ratio is feasiblity at 3.5μm.

4. Conclusion

We propose an ultra-compact, low loss, broadband and high extinction ratio PBS integrated on SOI platform employing polarization sensitivity of surface plasmon polariton. The device requires a straight forward fabrication procedure and is well suited for on chip dual polarization WDM systems.

Acknowledgements: The authors acknowledge support from the Karlsruhe School of Optics & Photonics (KSOP), the Center for Functional Nanostructures (CFN) and the German Research Foundation (DFG), the NAVOLCHI EU-project and the Teratronic school of the Helmholtz Association.

5. References

[1] http://www.ozoptics.com/
[2] C. H. Brown, inventor; 1940, US Patent 2.224.214
[3] Xianyu Ao et al., Opt. Lett. **30**, 2152 (2005)
[4] Wissem Sfar Zaoui et al., in *6th SODC,*(2010)
[5] Yao Zhang et al., Opt. Commun. 283 (2010) 2140–2145
[6] T. K. Liang et al., IEEE Photon. Technol. Lett., **17**, 393 (2005)
[7] Dirk Taillaert et al., IEEE Photon. Technol. Lett., **15**, 1249 (2003)
[8] Huaming Wu, et al., J. Opt. **12** (2010) 015703
[9] Chao-Yi Tai et al, IEEE Photon. Technol. Lett., **19**, 1448 (2007)
[10] C.-L. Zou et al., Opt. Lett. **36,** 3630 (2011 September 15)